Tides as triggers of earthquakes in Hindu Kush II.

Lubor Ostřihanský
Nad Palatou 7
150 00 Prague 5
Czech Republic
ostrh@tiscali.cz

Abstract
The intermediate-depth earthquakes (~200 km) in Hindu Kush, Afghanistan were investigated to prove their origin by tides. An untraditional astronomical method has been used to prove how astronomical parameters influence triggering of earthquakes. In contrast to previous issues, where Moon hour angles were used, Moons declinations were used successfully to prove tidal origin of earthquakes. Maximum earthquakes have been recognized during minor lunar standstills, i.e. in periods 2014-2015 and 1997-1998. Except of this, next strong earthquakes periodicity has occurred in period 1983-1984, 2001-2002 and 2021-2022 close to major lunar standstill.

Keywords Hindu Kush Earthquakes, Tidal forces, Earth rotation variations, Astronomical parameters: Moonrises, azimuths, Moon hour angles and declinations, Major lunar standstills, Minor lunar standstills

Introduction

The paper under the same title has been elaborated already in 2015 for GET Conference in Trieste (Ostřihanský 2015a) and presented with corrections on AGU Fall Meeting in San Francisco 2016.(Ostřihanský 2016a).Because many important earthquakes have occurred since that time, new issue has been prepared summarizing new achievement to prove tidal origin of earthquakes. Previous issues comprised comprehensive treatise, how many attempts have been made to prove or disprove earthquake triggering by tides in the past 100 years. This will be omitted in this issue and new important results of past 7 years are presented. Except of this new mathematical relations of tides are presented and new methods of elaboration suggested.

There is no doubt that the strongest earthquake Sumatra 2004 has been triggered by tides (Ostřihanský 2015a)..It occurred in Full Moon and maximum tidal torque corresponding to large declination 27º and also large Sun.s declination close to winter solstice. This exceptional configuration for maximum tidal effect is evident from Figs at the end of next paragraph. In Sumatra earthquake triggering occurred again in next New Moon but next earthquake occurring after 14 days in next Full Moon has been outside maximum tidal torque. Solution conveyed investigation of earthquake Sulawesi (Ostřihanský 2019a). In spite that Sulawesi is from Sumatra in distance 2000 km, earthquake in New Moon occurred exactly in maximum tidal torque. Exact position has been done by no existence of subduction zone in vicinity of Sulawesi Palu Koro Fault, whereas Mentawai Fault in Sumatra is situated above subduction zone. This revealed next important tidal torque acting westward perpendicularly to north-south torque, pushing IndoAstralian plate northward. Calculation of both tidal torques are presented in next paragraph. Action of both tidal torques presented tool, why to many authors tidal estimation of earthquakes presented negative results (Ostřihanský 2018). Even controversial problems have been solved, for example why on Sumatra 2009 in winter solstice maximum tidal torque in Full Moon no earthquake occurred. Solution conveyed rapid westward movement of plate by gravity to subduction zone. (Ostřihanský 2020a). In detailed study of earthquake in Central Italy, repetitions of maximum earthquakes have been discovered in 18.61 years Moon nodal period (Ostřihanský 2016c,d) occurring in minimum lunar standstills and also similar repetitions in Alaska with maximum lunar standstill. For Central Italy prediction of earthquake has been suggested for 2034 (Ostřihanský 2016e) and

for Alaska for 2021 (Ostřihanský 2017a)..This has been the greatest author's success, when this prediction has been fulfilled (Ostřihanský 2021b). Investigation of devastating earthquake in Nepal of Gorkha earthquake 2015 revealed resonance effect for earthquakes triggering and devastating earthquake in 1934 has been attributed tu tides (Ostřihanský 2015c).. Earthquake on Taiwan 26.12.2006 confirmed tidal westward tidal movement of Philippine Plate (Ostřihanský 2010a) and explained formation of obduction (Ostřihanský 2018)..Obduction has been explained as impossibility of subduction of mid-ocean ridge oceanic material. Development of Indian Ocean has been described in (Ostřihanský 2015) and collision between India and Asia in (Ostřihanský 2020b) resulting in tidal development of Himalayas, explaining position of deep oceanic sediments in top of Himalayas by obduction of mid-ocean ridge of Tethys. Formation of it has been explained by movement of Gondwana and reciprocal movement of oceanic lithosphere by tidal torque. Earthquake on Haiti M 7.2 14.VIII.2021 (Ostřihanský 2021a) with paper about Haiti earthquake 2010 (Ostřihanský 2012a.b) presented tool of identification of westward and north south tidal torques and explained origin of predicted earthquake Chignik Alaska 29.V. 2021 (Ostřihanský 2021b) and following earthquake in Alaska Gulf M 6.9 14. VIII/ 2021. Last papers (Ostřihanský 2020a) and (Ostřihanský 2022b,c) explained tidal origin of earthquake and structure of mantle and existence of subduction and permanent action of hotspot plumes.

No wonder that the author could not omit discussion of devastating earthquake in Afghanistan south of Kabul M 6, 21.VI.2022, summarizing old results of previous Hindu Kush investigation directing on positions of earthquakes on tectonic faults, using available tectonic and geologic maps of Afghanistan.

For investigation three periods of strongest earthquakes were chosen: 1983-1984, 1997-1998, 2001-2002, 2014-2015 and 2021-2022. As has been shown, periods 1997-1998 and 2014-2015 are in time span of nodal Moon's 18.61 years period, the period of lunar minor standstills when Moon's declination is only ±18°, being close to equator, exerting maximum decelerating torque. The importance of Moon's nodal period has been discovered in author's investigations of periodicity of earthquakes in Central Italy (Ostřihanský 2016c) and finally presenting reliable prediction of earthquake for autumn 2034 in Norcia-Marche-Abruzzi region (Ostřihanský 2016d).

How tides drive lithospheric plates

In 1991 the author (Ostřihanský 1997, 2015a) derived the map from the no net rotation frame, but the zero point of the plate movement was chosen on the northern side of the Nazca plate in coordinate 5°S and 90°W. The movement of plates was divided into northward and westward components (Fig. 1).

The northward component was attributed to tides because tidal torques directing northward (Fig. 2) are sufficiently strong (Ostřihanský 2015a). Broz et al (2011) calculated for Moon 1.2 $\times 10^{22}$ Nm and for Sun 5.7 $\times 10^{21}$ Nm, using in both cases the same obliquity to equator 23.45°, The ratio of tidal action of Moon and Sun is approximately 2:1. The Sun has the 48 % share in tidal action. For this reason the share of Sun is very important for earthquake triggering and also for the plate movement. The most devastating earthquakes in the Indian plate, the great 1934 Nepal earthquake was triggered in New Moon (Ostřihanský 2015c).and 2004 Sumatra earthquake in Full Moon (Ostřihanský 2015a).

Dominant movements on the Earth are the northward movements, evoked by north-south tidal torques,. Owing to obliquity of Earth rotation axis, tides drift out of equator all continental and oceanic plates. Not Wegener's Polfluchtkraft but ëquator-flucht (equator-fleeing force) is dominant force driving plates. Diurnal and Moon's sidereal (27.56 days) variations together with Moon nodal (18.61 years) are dominant variations driving plates, either northward, because at present time subduction is possible only on northern hemisphere

and facilitate westward movement by mechanism overcoming friction of weak tidal friction torque10^{16} Nm by perpendicular variations of ëquator-flucht 10^{22} Nm (Fig. 2).

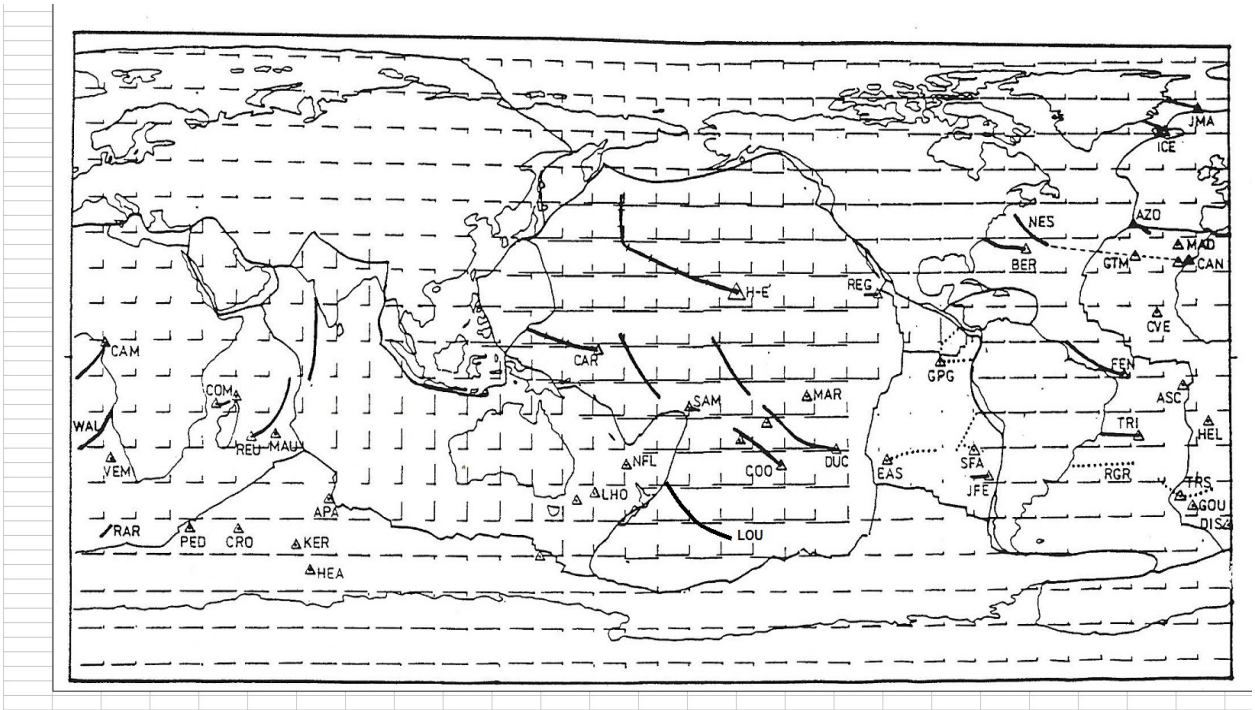

Figure 1. Minster and Jordan (1978) established imagination of no rotation frame, according which lithospheric plates moved chaotically against each other or dispersed in mid-ocean ridges supporting imagination of mantle convection. Because small plates as Nazca and Cocos remain stable on mantle, then calculation shows that plates move in direction of westward and northward components as depict on figure. Solid curves depict hotspot tracks, which show that originally plates moved northward (Reunion hotspot (REU), disrupted by mid-ocean ridge. Original movement of Hawaii-Emperor Seamount Chain (H-R) has been also northward but later prevailed westward component. New England Seamount (NES) shows interruption of hotspot track by Mid-Atlantic Ridge and hotspot stable position in Canary Island (CAN), (Ostřihanský, 1997).

There are some differences in movement of north and south hemispheres. The movement of the Eurasian and North American plates demonstrates the westward movement of northern hemisphere. The movement of Eurasian plate is documented by opening of back-arc basins on its eastern side, where subducting oceanic lithosphere of the Pacific plate is firmly in mantle anchored in Kuril Trench, Japan trench, Nankai Trench, Ryukyu Trench, and Philippine trench. Eurasian plate receding westward opens behind itself oceanic lithosphere of these basins. Slow differences in westward movements of Eurasian and North American plates is evident on narrow opening of Atlantic ocean, but quick movement of both plates is evident from overriding the East pacific Rise.

- Plates at present move northward, not southward, because after the decay of Gondwana, the oldest and heaviest oceanic lithosphere remained along southern rim of Laurasia, prone to subduct by gravity descent.

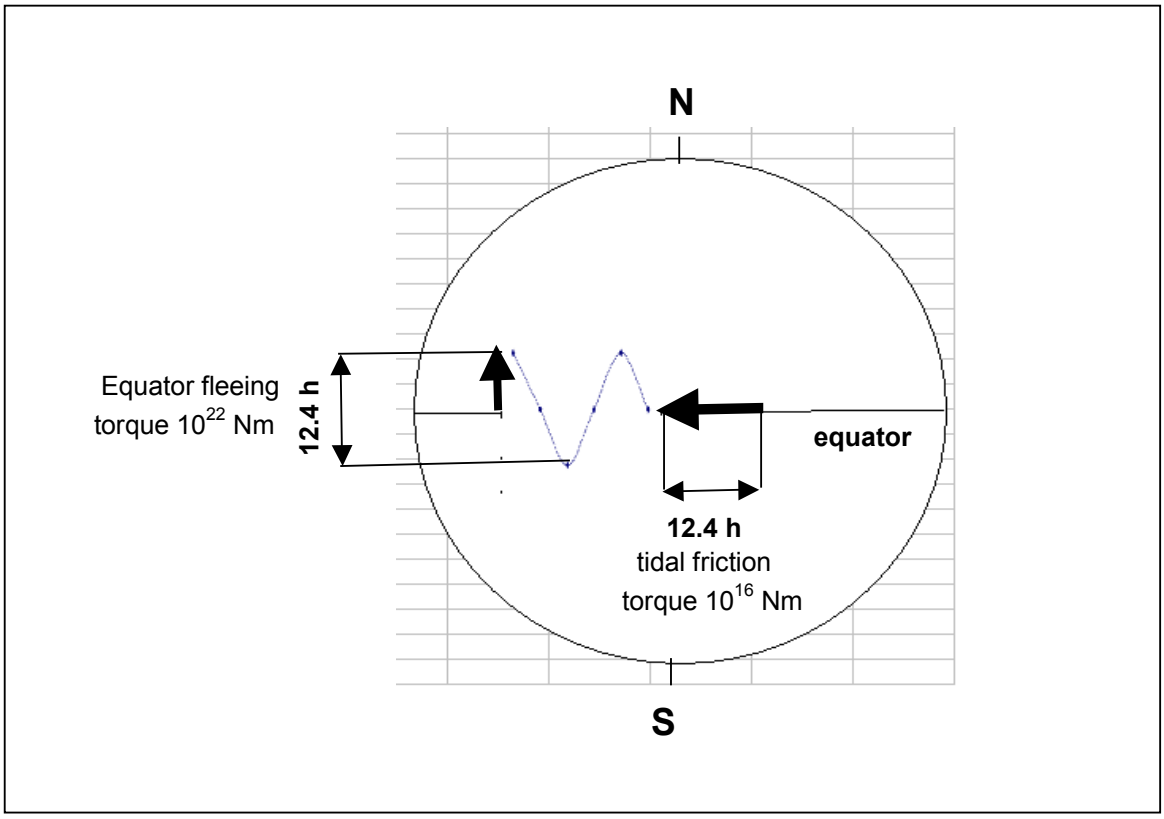

Figure 2. The whole lithosphere is subjected to two perpendicularly acting forces: tidal friction 10^{16} Nm and equator-fleeing directing north 10^{22} Nm. By permanent action of these forces acting in 12.4 h period (Moon 12.42 h, Sun 12 h) the whole lithosphere moves westward. (Half value of equator-fleeing force concerns plates moving northward, because southern component is damped in mid-ocean ridge, which acts as ratcheting mechanism). Extremes on periodic curve of figure are maximum and minimum stresses of Moon acting on equatorial lithosphere calculated from equation (2) with periodic addition or subtraction of stress of Sun (equation 1). On lithosphere act both forces, zonal north-south equator flying and westward drift which decelerates the Earth rotation (Lambeck, 1977).

Tidal forces acting on plates are following:
1.Forces, which try to align the Earth's flattening to the level of acting tidal forces, i.e. to the planes of Moon and Sun orbits.
2.Force, which brakes the Earth's rotation, i.e., the tidal friction.

1. Fig. 3 shows the action of the tidal force in its most effective action during the Sumatra earthquake 2004. The torque acting on the plate can be calculated in following steps (Brož et al 2012):
Earth's angular velocity $\omega = 7.29\ 10^{-5}$ rad/sec, Earth's moment of inertia $I = 8.036\times 10^{37}$ kg m^2 (Stacey and Davies, 2008). Earth's angular momentum $L = I\times\omega = 5.89\times10^{33}$ kg m^{2}s^{-1}. Mass of the lithospheric bulge is

$$m_{bulge} = \frac{1}{2}\left(\frac{4}{3}\pi abc - \frac{4}{3}\pi c^3\right)\rho_{crust},$$

where we insert $a = b = R_e \approx 6378$ km, $c = R - 21$ km, $\rho_{crust} \approx 2700$ kg m^{-3} and we get $m_{bulge} \approx 9.6\times10^{21}$ kg $\approx 1/624\ m_e$. (Earth's mass $m_e = 5.97_{\,x}\ 10^{24}$ kg). The torque of force couple

acting on the Earth is then: in case of the Sun (m_s, r_s Sun's mass and distance, G gravitational constant)

$$M_s = 2 \times \frac{2Gm_{bulge}m_s}{r_s^3} R_e \cos\varepsilon . R_e \sin\varepsilon \ , \qquad (1)$$

where ε = 23.45° is the obliquity of ecliptic to equator. This is valid only in case if the mass of bulge were concentrated in one point on equator and the Sun were just in highest point above equator. In reality we should integrate over the bulge because some its parts are closer to the axis of rotation and to center over the Earth's rotation because the instant angle of the Sun above equator varies. We would get:

$$\overline{M}_s = \frac{1}{4} M_s \approx 5.7 \times 10^{21} \text{ N m}$$

The same calculation is for the Moon:

$$M_m = 2 \times \frac{2Gm_{bulge}m_m}{r_m^3} R_e \cos\iota . R_e \sin\iota \ , \qquad (2)$$

where τ is the Moon's declination (insert 23.45°). The result is $\overline{M}_m = \frac{1}{4} M_m \approx 1.2 \times 10^{22}$ N m. The torques simply summarize $\overline{M} = \overline{M}_s + \overline{M}_m = 1.8 \times 10^{22}$ N m.

This important result calculates that the torque 1.8×10^{22} N m is able to move the plate in north-south direction. The seismic moment of the Sumatra earthquake is 3.5×10^{22} N m (Varga and Denis 2010; Lay et al 2005; Stein and Okal, 2005). Because the torque exerted by tidal force acting on Earth's flattening represents the kinetic energy and also the seismic moment represents energy according to definition $M_0 = \mu AD$, where μ is the shear modulus N/m^2, D is displacement on area A, this quantity of N m dimension represents also energy, both quantities can be compared.

2. The torques of tidal friction were calculated by Burša (1987a), (1987b) on the basis of angular momentum balance in the Earth – Moon – Sun system.

$$N_m = 4.2 \times 10^{35} \text{ kg m}^2 \text{ cy}^{-2} = 4.2 \times 10^{16} \text{ kg m}^2 \text{ s}^{-2} = 4.2 \times 10^{16} \text{ Nm} \qquad (3)$$

$$N_s = 8.9 \times 10^{34} \text{ kg m}^2 \text{ cy}^{-2} = 8.9 \times 10^{15} \text{ kg m}^2 \text{ s}^{-2} = 8.9 \times 10^{15} \text{ Nm}$$

The ratio of tidal torques of Moon and Sun therefore is

$$N_m/N_s = 4.7$$

According to Jeffreys this ratio is 4.9 (Jeffreys 1975). The Sun's share in tidal friction is only 21%.

The tidal fiction decelerates the Earth's rotation (Lambeck, 1977) and therefore it can be also considered as the force causing the westward movement of plates (Ostřihanský 2012a,b).

The torque exerted by the tidal friction is relative low 10^{16} N m. (Burša 1987a) and considering the mantle viscosity only 2 orders of magnitude lower than the lithosphere (Cathles 1975), this force is considered as insufficient for the plate movement. But considering variable force (ad 2), acting on Earth's flattening, and tidal friction (ad 3) acting semidiurnally, then the westward movement is possible, owing to the north-south varying force ad 2, acting on it perpendicularly.

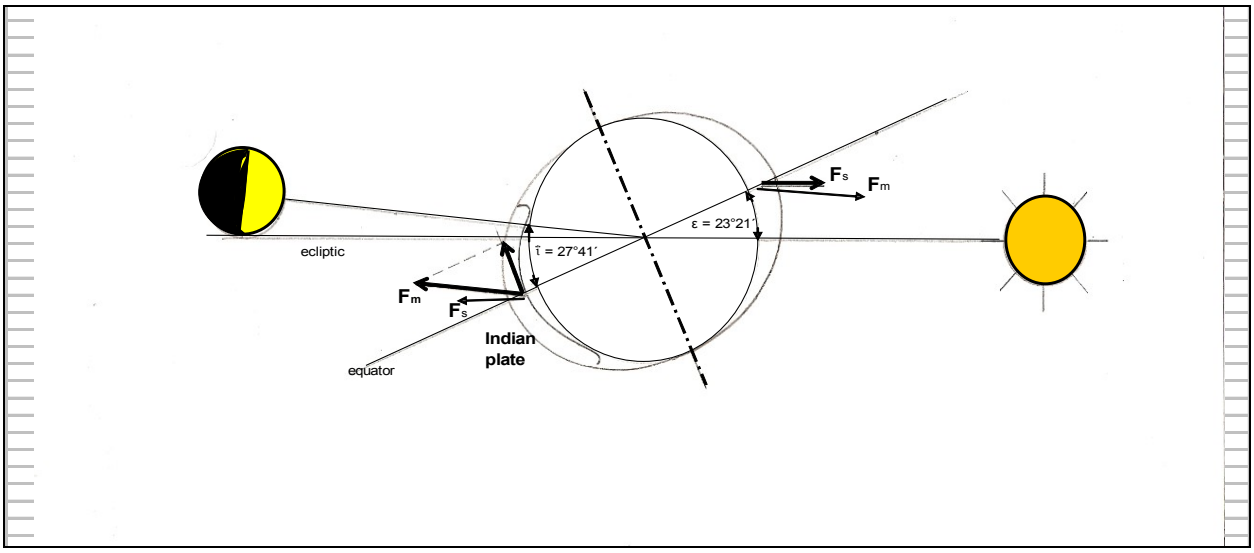

Figure 3 shows Full Moon, maximum Moon's declination 27º 21´ and the torque acting on Indian plate directs northward. 12.4 hours later torques direct southward (not marked in figure) against mid-ocean ridge and no earthquakes are triggered. This is the case of Great Sumatra earthquake 2004. Moon's torque (F_m=M_m) directs northward and also the Sun's counterpart S_c=F_s), as evident in wintertime.

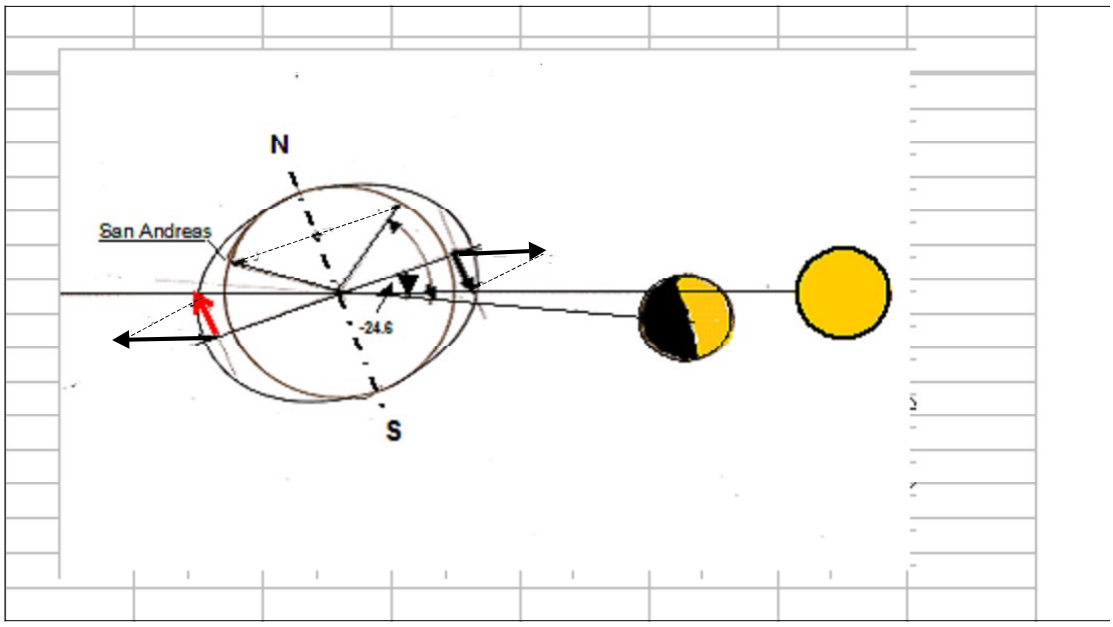

Figure 4. Case of New Moon in winter, when Sun's and Moon's declinations are negative (Moon –24.15º), but earthquakes are triggered for 12.4 hours later (marked by red arrow). Black arrow direct southward against mid-ocean ridge without any earthquake or the plate movement. Therefore, Moon and Sun counterparts cause northward plate movement.

Hindu Kush "intermediate-depth" earthquakes zone, Earth's rotation variations and periodic repetitions of earthqaukes in 18.61 years cycle

Whereas this isolated deep seated earthquake zone of depth about 200 km represents for supporters of mantle convection an unsolvable mystery, the author (Ostřihanský 2015a) explained the mechanism (Fig. 2) of earthquake triggering in this zone quite simply. Owing to

westward movement of the Eurasian plate (Fig. 1), the part of subducted oceanic lithosphere of the Indian plate was torn off and shifted for several hundreds kilometers westward. Cross-sections through the Hindu Kush region suggest a near vertical northerly-dipping slab (Negredo et al., 2006, Searle et al., 2001, Searle 2013) firmly kept in lithosphere. Such body should be extremely sensitive to daily action of westward tides driving Eurasian plate, but also northward acting variable torque of Indo-Australian plate intervening also to this site. As explained in model (Fig. 2) this variation increases in Moon sidereal cycle 27.56 days reaching ±28º Moon's declination, but also in 18.61 years cycle varying from maximum 28º to minimum only 18º. Maximum declination is called major lunar standstill and minimum, minor lunar standstill..

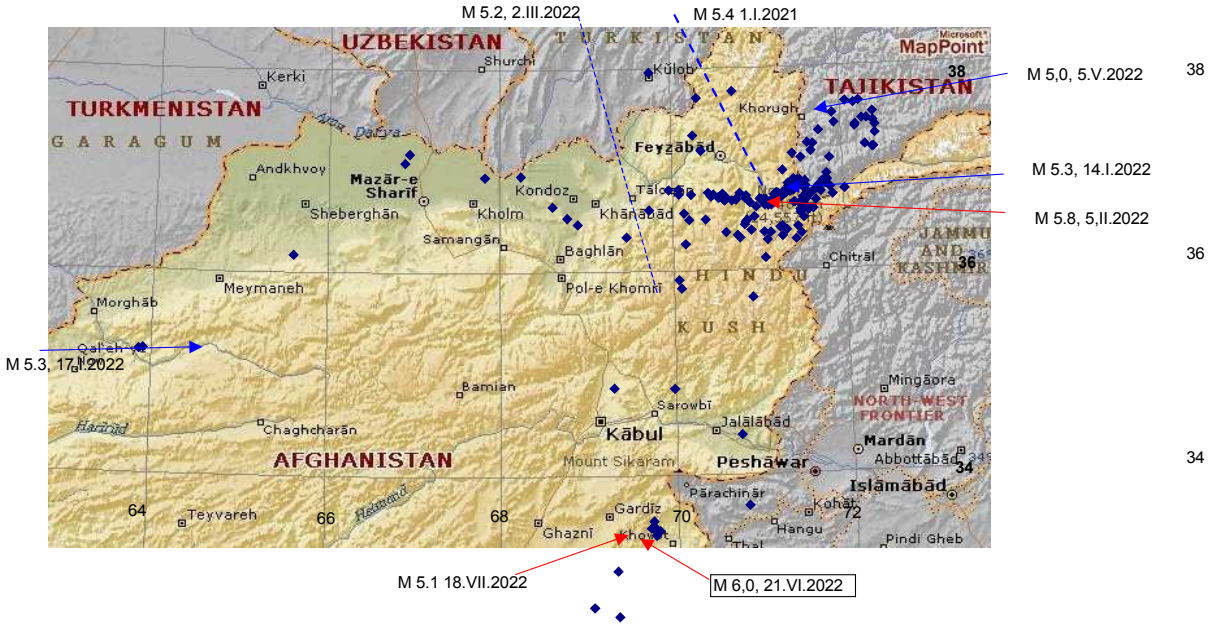

Figure 5. shows northern part of Afghanistan with earthquakes in 2022**.** . Devastating earthquake M 6, 21.V.2022 is in rectangle. Red arrows mark triggering by westward, blue arrows northward directing tidal torque respectively.

Earthquakes selected from this area (Fig. 5) from Afghanistan and adjacent areas of Pakistan and Tajikistan cover the zone of the deepest earthquakes of Hindu Kush and confirm the westward tidal movement and northward alternating movement evoked by Moon\s variable movement along equator, i.e. Moons variable declination. Figs. 10A, 11A, 12A, 13A and 14A show the plot of earthquakes and Earth's rotation variation expressed as the length of day variations (LOD).

Choosing maximum magnitude earthquakes, it is possible to find two earthquake groups, first repeating in minimum Moon's declination ±18º after 18.61 years (minor lunar standstill) and group of maximum Moon's declination 28º, repeating again after 18.61 years. First group occurred in 1997-1998, 2014-2015 with prediction 2034, the second one 1983-1984, 2002-2003 and last as successively predicted in 2021-2022. The first repetition has been recognized first in Central Italy .(Ostřihanský 2016), the next in South-Central Alaska .(Ostřihanský 2017). Existence of two groups reflects complicated situation in collision of two plates westward Eurasian and northward Indo-Australian. Maximum earthquakes in maximum lunar standstill are for 5 years shifted owing to north-west movement of plates.

Proof of earthquakes triggering by tides

First attempt to prove tidal origin of earthquakes has been made choosing Moon's hour angles in time of earthquakes and calculating Moon's hour angles from Moonrise over horizon up to Moon's hour angle in time of earthquake. Choosing all possibilities, when Moon has been below

horizon, the Moon's counter part has been chosen by adding 180º to hour angle. Constructing histogram from all earthquakes from 2021-2022 earthquake group (Fig. 10A), i.e. 126 earthquakes, Fig. 6 presents result:

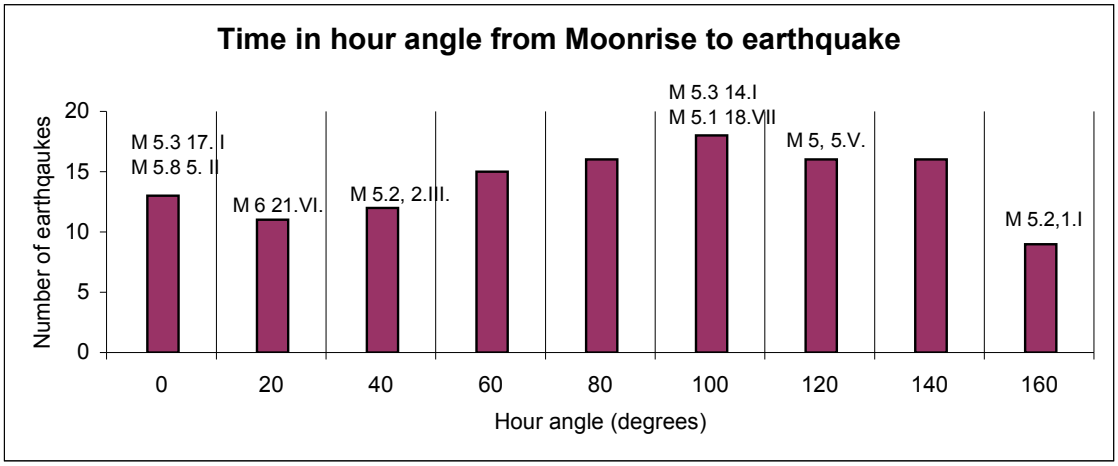

Figure 6. Histogram of number of earthquakes in Moon's hour angle distance from Moonrise.

Histogram simply shows that maximum earthquake occurred under hour angle 90º, i.e. when Moon is in meridian. For Moonrise special formula has been used stemming from spherical triangle, knowing Moons azimuth A and z as zenith distance in horizontal coordinates and looking for declination δ and hour angle t, which will be compared with positions of earthquakes in equatorial coordinates and given longitude φ.
This problem solves equations

$\sin z \sin A = \cos \delta \sin t$
$\sin z \cos \delta = -\sin \delta \sin \varphi + \cos \delta \sin \varphi \cos t$
$\cos y = \sin \delta \sin \varphi + \cos \delta \cos \varphi \cos t$

Looking for Moonrise then z - 90º and equatiionsare simplified as

$0 = \sin \delta \sin \varphi + \cos \delta \cos \varphi \cos t$
and for Moon rise t is valid $\operatorname{cotg} t = -\operatorname{tg} \delta \operatorname{tg} \varphi$.

For practical calculations using adjustments, formula can be used:

$$tg\frac{t}{2} = \pm\sqrt{\frac{\sin(\varphi - \delta)}{\cos(\varphi + \delta)}}$$

(Almucantharates above horizon are smaller with negative declination and larger with positive declination. In statistics both sizes are equilibrated)

Far better results, Moon's **declination** is more suitable**:**
Simply plot of histogram (Fig.7) shows bimodal character. First maximum is at declination 0º and two next at maximum Moon declination ±25º on both sides of graph. corresponding to year 2022 declination

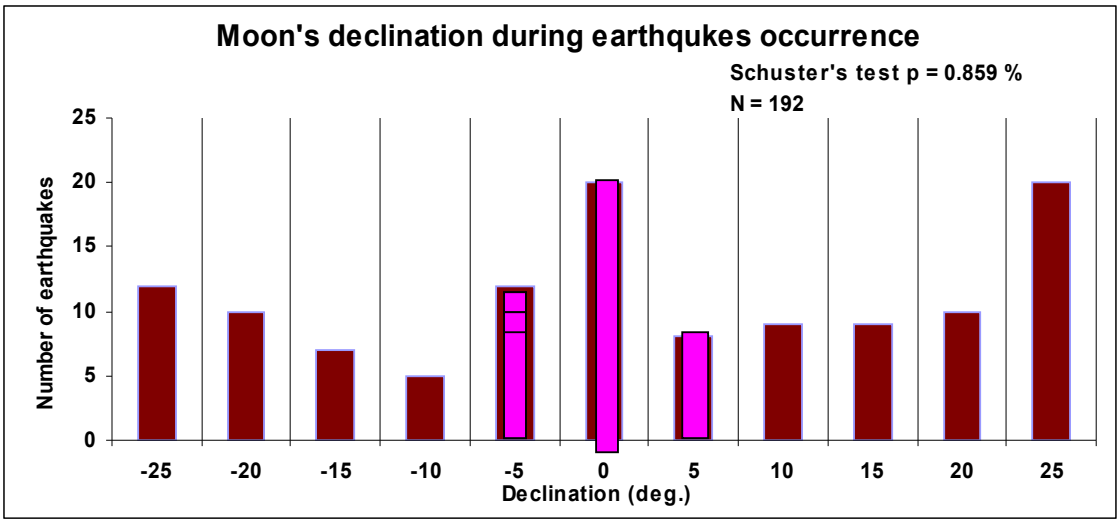

Figure 7. Histogram of number of earthquakes during Moon's variable declination for group of earthquakes of 2022. Purple red earthquakes triggered under Moon's declination ±7.5º correspond to maximum westward directing tidal torques..

Purple red dots mark positions of Moon's ±7.5º declination earthquakes with maximum westward tidal torque acting along equator with declination 0º. Purple red earthquakes follow westward directing fault HR and HM and northeast directing PJ (Fig 8). Purple red earthquake is also south of Kabul (bottom part of figure), the exceptional site where in 10 km depth devastating earthquake M 6, 21.VI. 2022 has occurred.

Comparison of earthquakes (marked by purple red), which were triggered by westward directing tidal torque with real tectonic faults, presents the best ever made proof of triggering of earthquakes by tides.

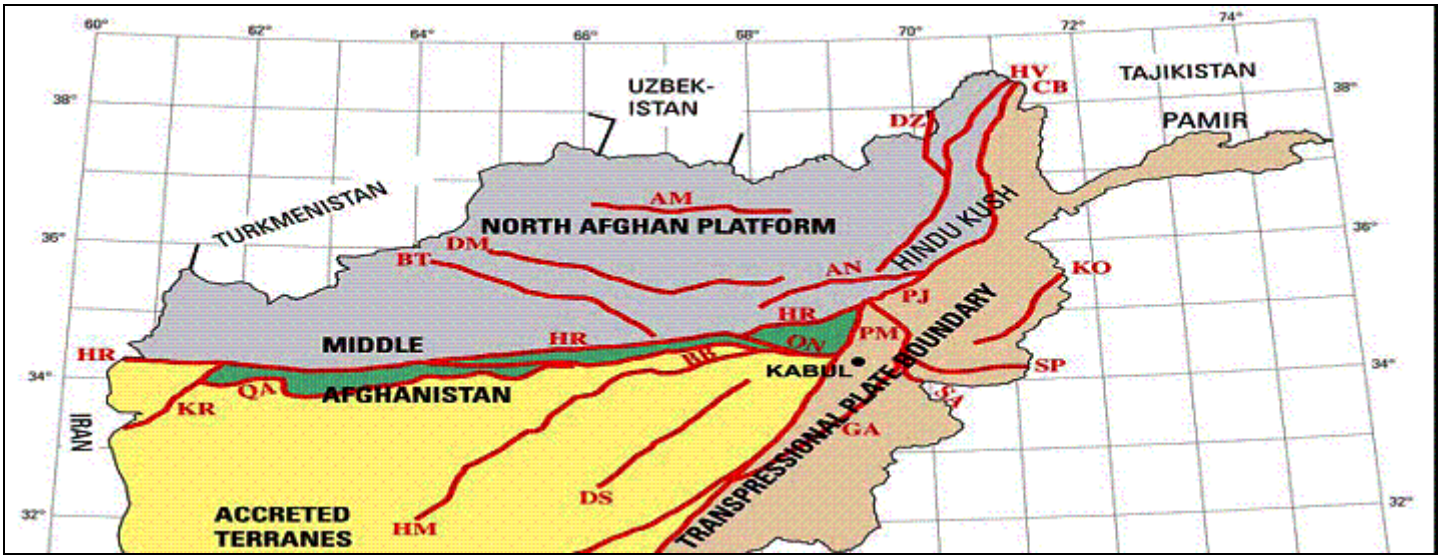

Figure. 8. Seismotectonic provinces and major fault zones (bold red lines). Abbreviations of fault names: AM, Alburz Marmul; AN, Andarab; BB, Bande Bayan; BT, Bande Turkestan; CH, Chaman; CB, Central Badakhshan; DS, Dorafshan; DZ, Darvaz; DM, Dosi Mirzavalan; GA, Gardez; HR, Hari Rud; HM, Helmand; HV, Henjvan; KR, Kaj Rod; KO, Konar; MO, Mokur; ON, Onay; PM, Paghman; PJ, Panjshir; QA, Qarghanaw; SA, Sarobi; SP, Spinghar. Modified from Wheeler *et al.* (2005).

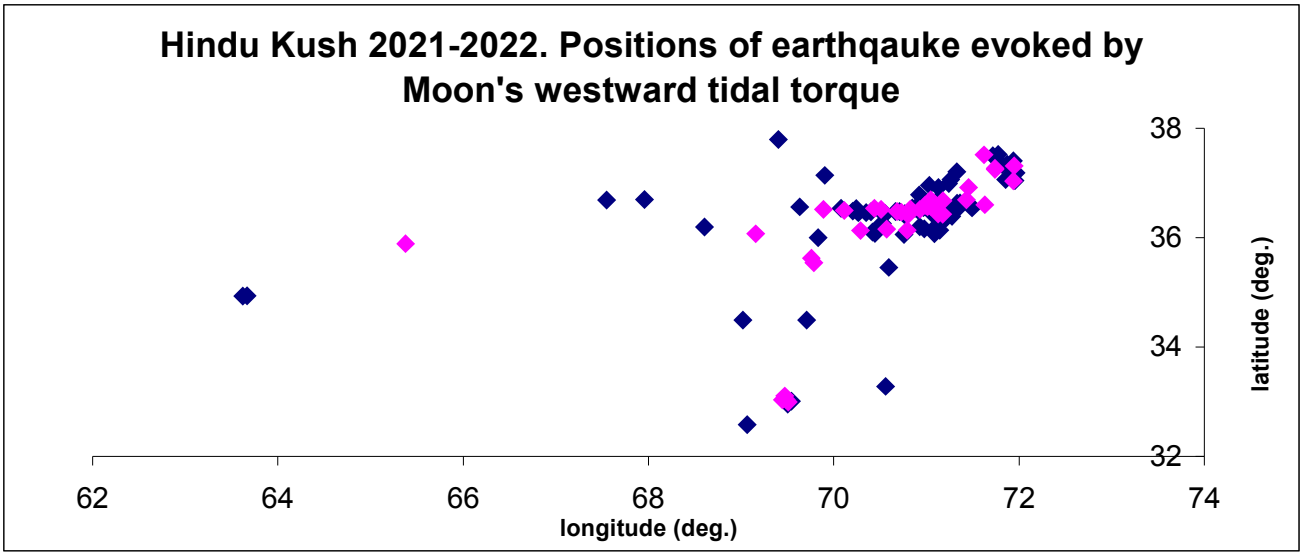

Figure 9. Comparison of plotted earthquakes evoked by westward tidal drag (purple red dots) with real tectonic faults in Hindu Kush presents the best ever used proof of tidal triggering of earthquakes.

Figure 9 shows evidently Hari Rud Fault (HR) created by westward movement and earthquake triggering (purple red dots) along this fault. Fig 8 shows evident westward movement area of west from Hindu Kush and ray-running (radial) faults from center of Hindu Kush trying to keep position. One of these faults is situated south of Kabul, the site of devastating earthquake M 6, 21.VI. 2022.(bottom purple red dot).

Comparison of Hindu Kush tectonics with earthquakes identified by LOD variations
Except looking up Moon's declinations, it is possible directly to use LOD extremes

1. **Earthquakes of major lunar standstill group.**

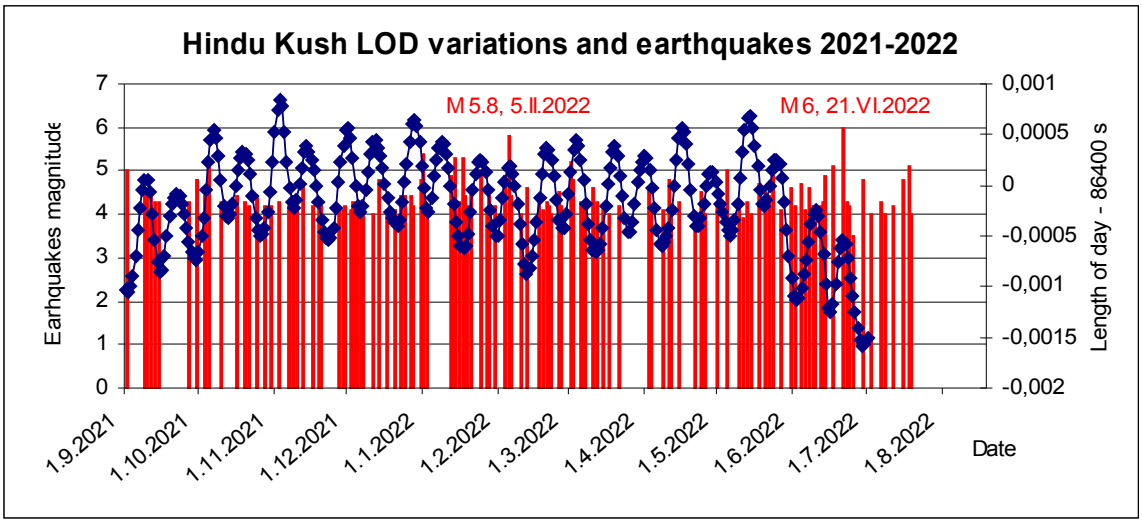

Figure 10A. Group of earthquakes has maximum magnitude earthquakes M 5.8, 5.II.2022 and M 6.0, 21.VI.2022 both situated on LOD maximums, corresponding to 0º Moon's declination. LOD minimums have alternating ± sign of declination + sign marks northward

movement, - sign southward movement (See eq. (1) and (2) for Moon and Sun. LOD marks summarizing effect including perigee distance.

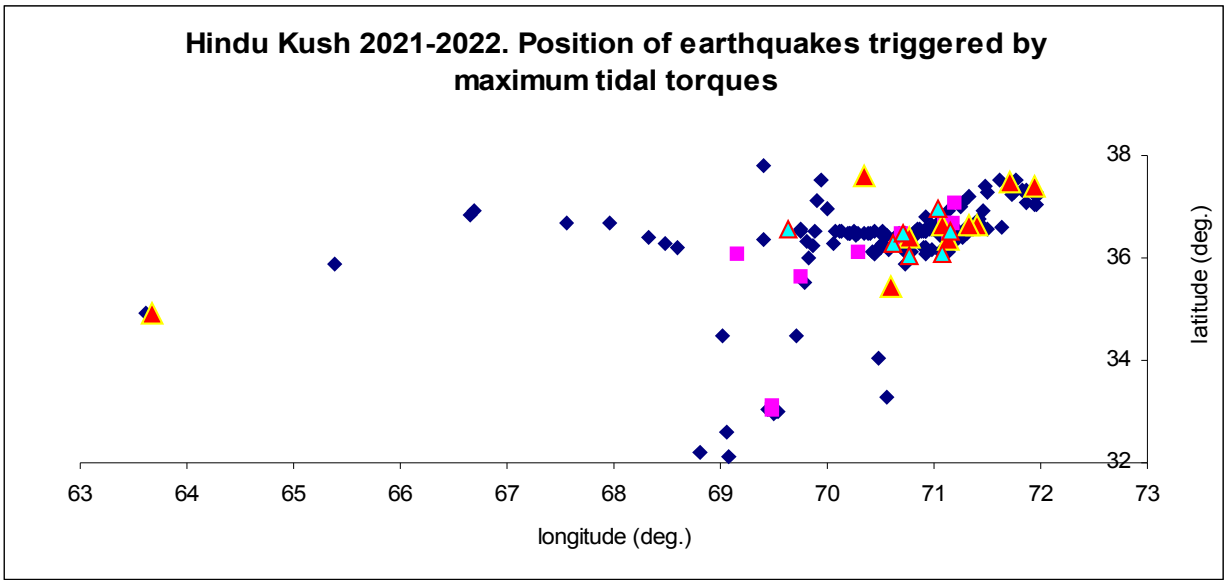

Figure 10B. Plot of earthquakes with extreme tidal torques: westward tidal triggering is marked by purple red squares, northward tidal torque by red triangles and southward blue triangles. It is evident; that northward tidal torque is dominant, whereas southward triggering remains fixed in center or in east-west directing fault.

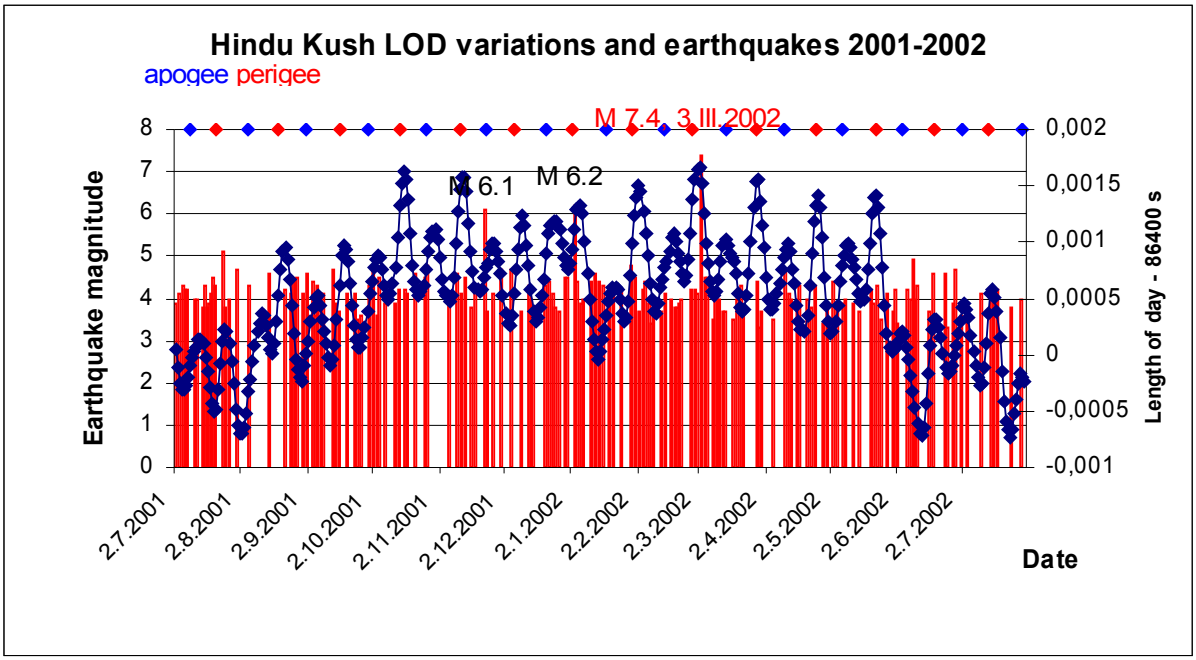

Figure 11A. Earthquake M7.4, 3.III.2002 dominates to this group in LOD maximum Earthquakes M 6.1 and M 6.2 do not correlate with any extremes of tidal torques of larger magnitude.

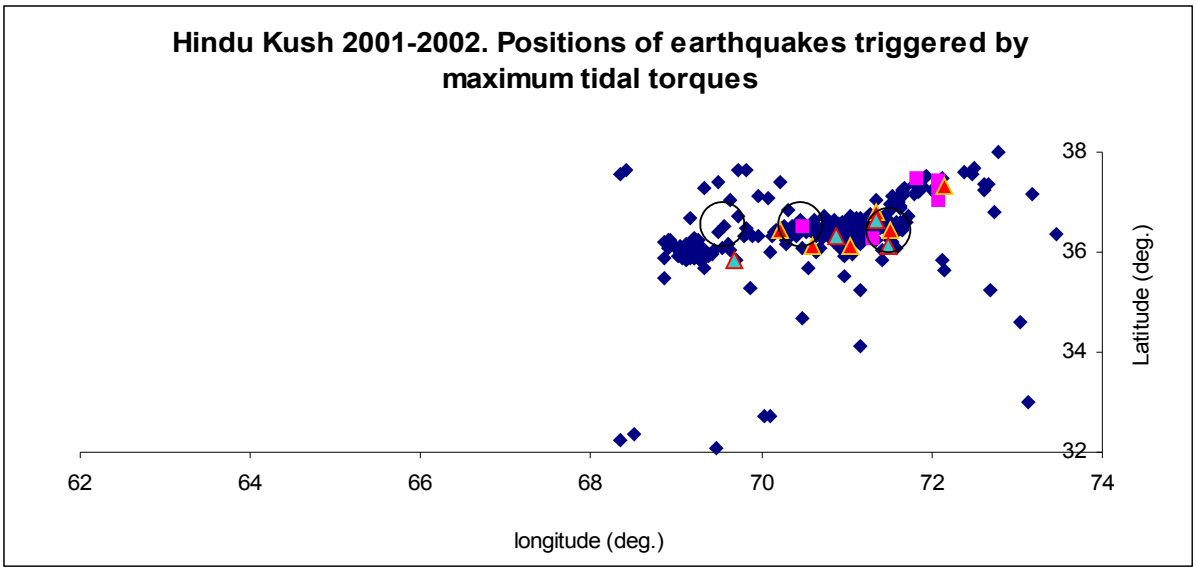

Figure 11B. Figure shows dominant westward tidal torque (purple red squares). Most earthquakes have no extreme values (dark blue dots). Large earthquake M 6.1 and M 6.2 are marked by circle. Circle between them marks large earthquake M 7.4, 3.III.2002.

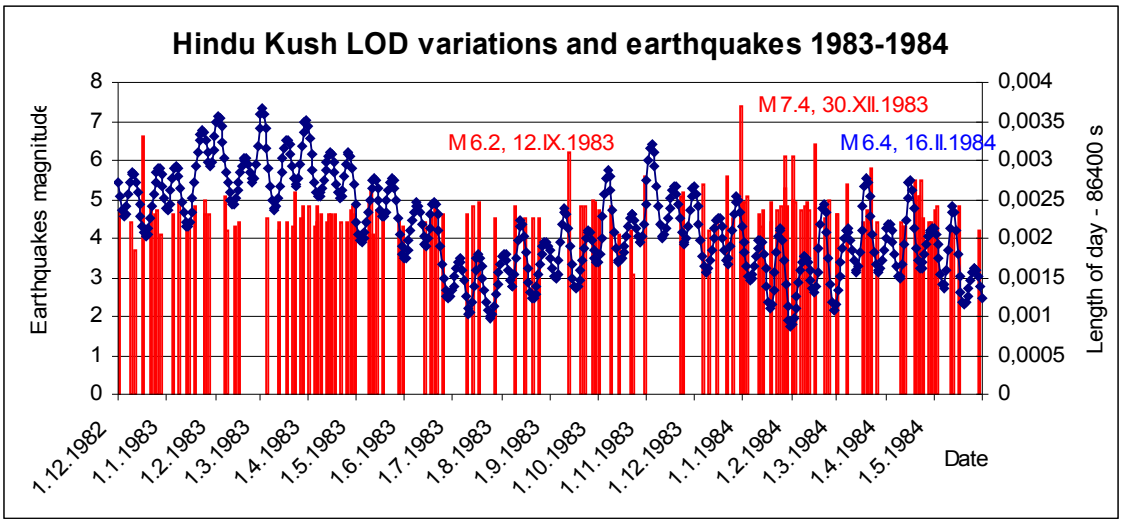

Figure 12A. This group has two large earthquakes M 7.4, 30.XII.1983 and M 6.2, 12.IX.1983 on LOD maximum and M 6.4, 16.II.1984 on LOD minimum (marked by blue color).

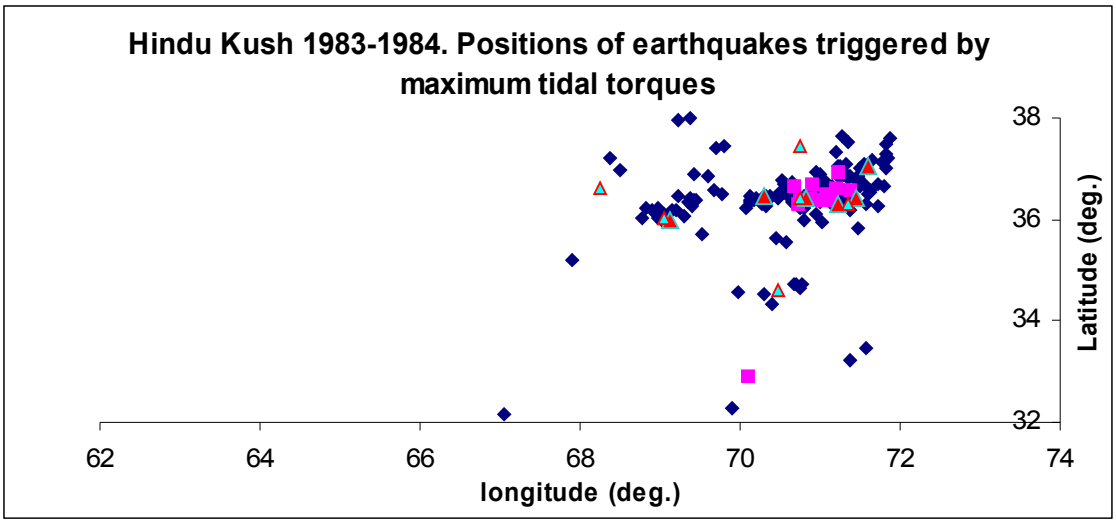

Figure 12B. M 6.4, 16.II.1984 has positive Moon declination situated in center swarm. Earthquakes with negative declination are scattered (blue triangles). This could convince about reciprocal movement southward.

2. Earthquakes of major lunar standstill group

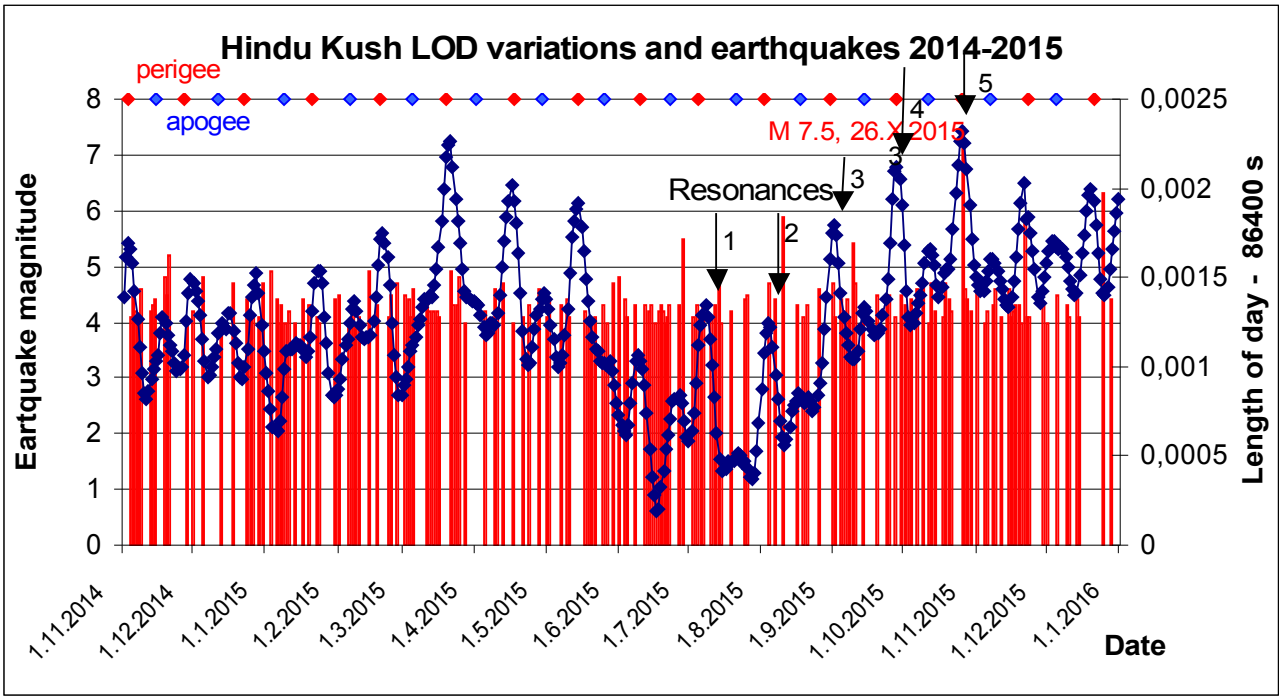

Figure 13A. Group has strong earthquake M 7.5, 26.X.2015 increased by resonance effect (numbers 1 – 5).

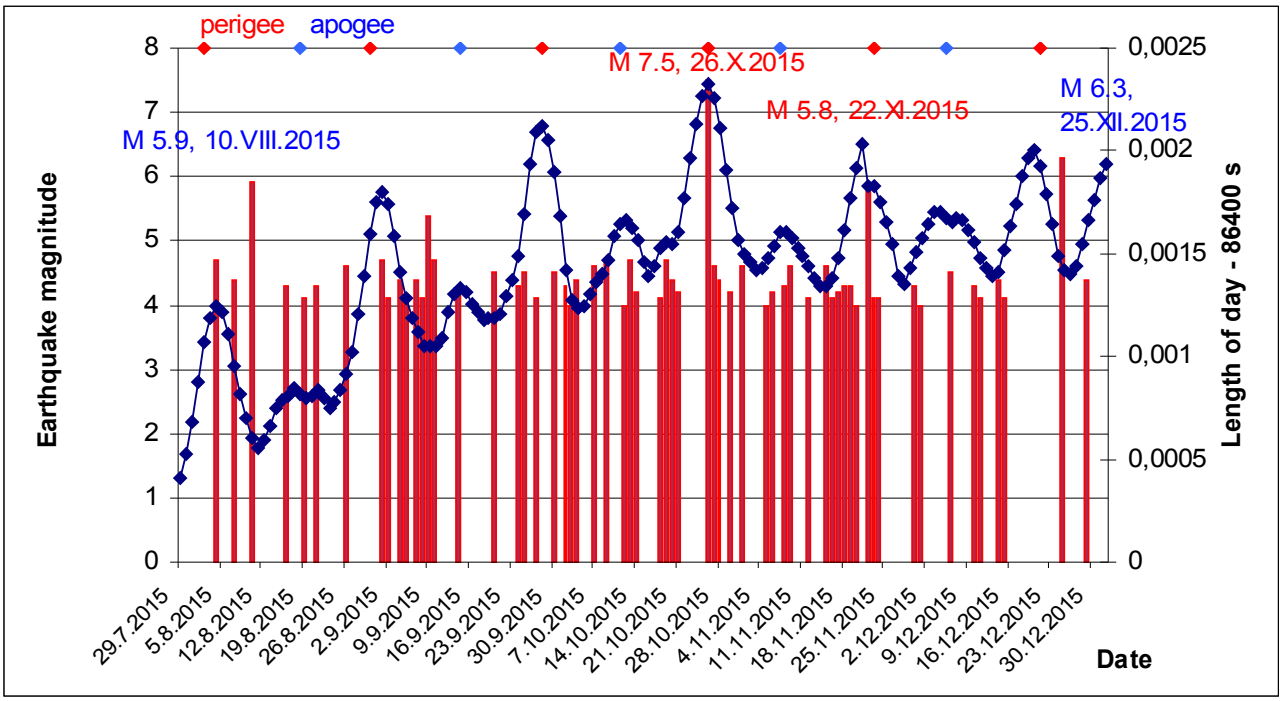

Figure 13A2. shows detail of earthquake M 7.5, 26.X.2015 with two earthquakes on LOD minimum (blue color)

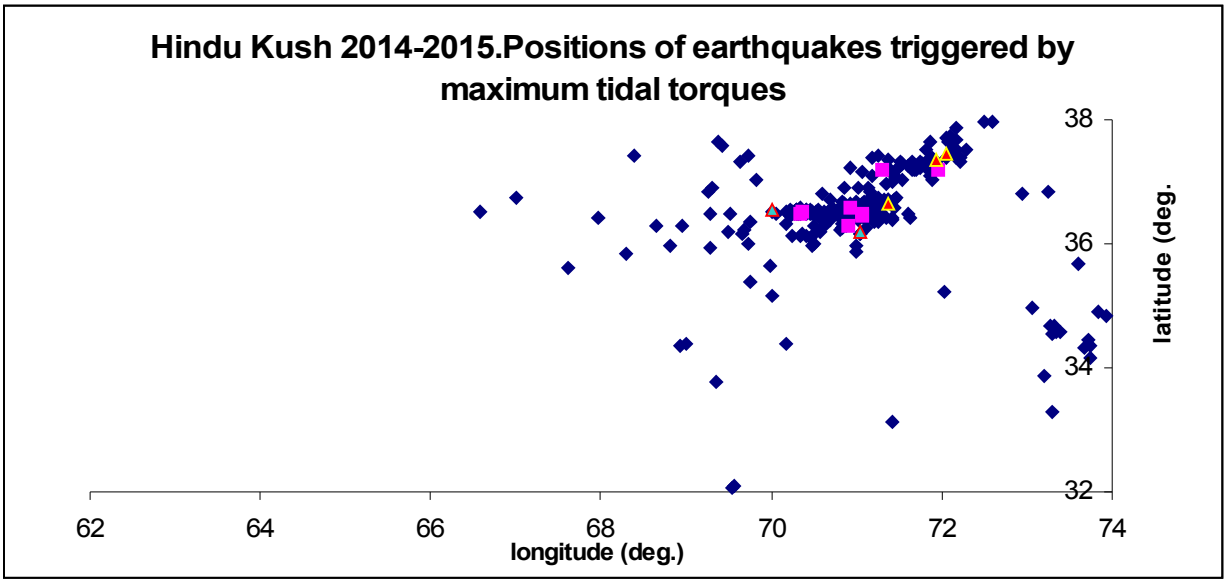

Figure 13B. Most of earthquakes with 0º declination (purple red squares) and negative declination (blue triangles) are concentrated in center of Hindu Kush. Positive Moon declination earthquakes (red triangles) direct north-east.

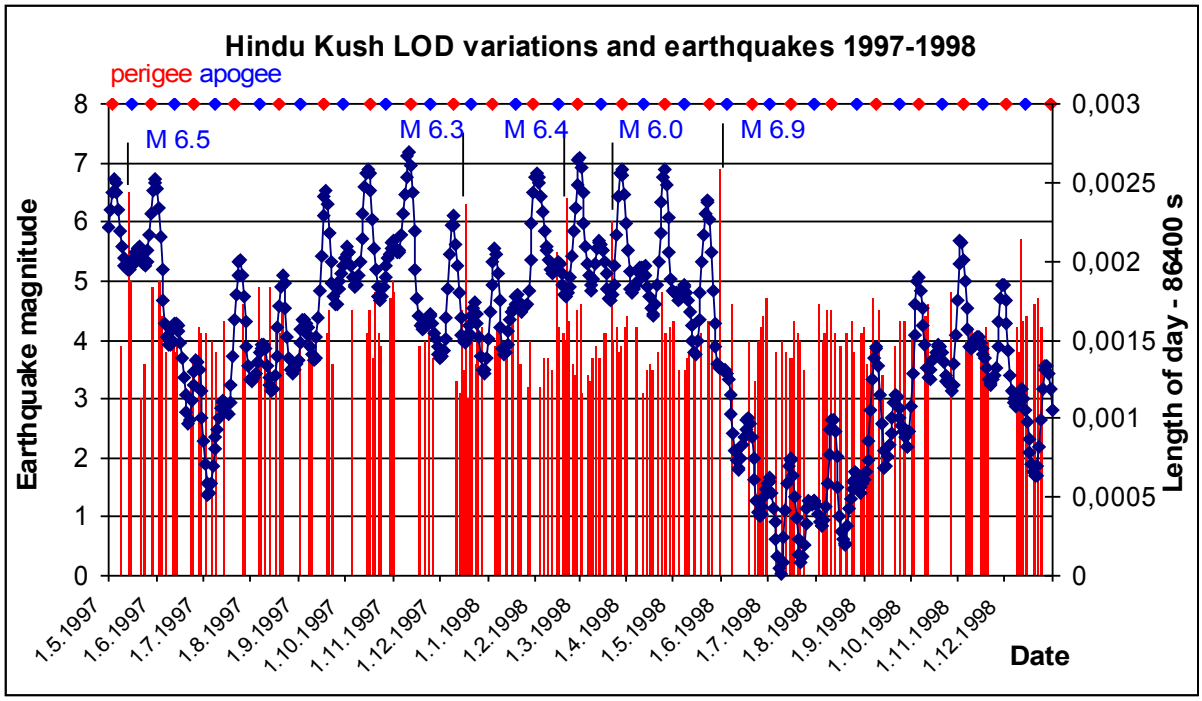

Figure 14A shows exceptional case of only earthquakes with maximum declination. of positive or negative sign.

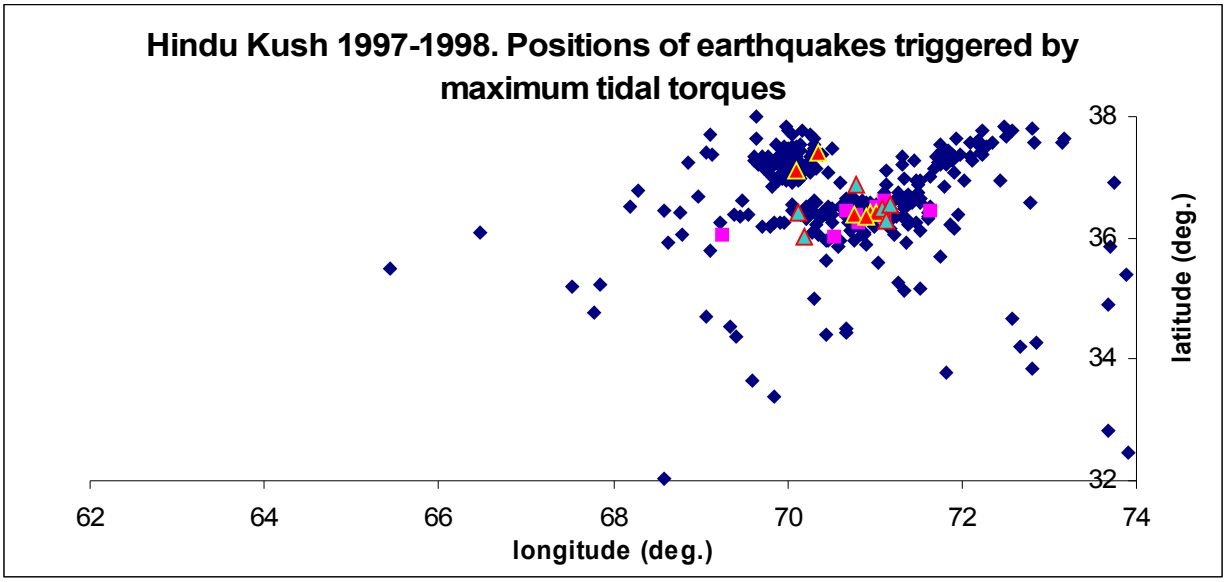

Figure 14B. shows positive declination earthquakes (red triangles) directing to north-west.

Conclusion

Positions of earthquakes triggered under 0º Moon's declination, situated on long westward directing fault, along which westward movement is evident, manifest the best proof of tidal triggering of earthquakes ever performed. Also maximum Moon's declination variations evoke northward plate movement provided free space is created in front of it. This confirms author's concept of lithospheric plates movement (Fig. 2) where lithosphere is subjected to north-south strong variations of 10^{22} Nm torque and permanent action of westward tidal drag. only 10^{16} Nm supported by north-south variations overcoming friction. Because Hindu Kush is subjected action of both tectonic movements westward and northward, there are two 18.61

years nodal Moon cycles, major and minor lunar standstills, with periodic increment of earthquakes.

Data acquisition

The ANSS Catalog Search has been used for all seismic data selected from rectangle 32°N - 38°N and 62°E - 74°E (500 x 1000) km in Afghanistan and adjacent part of Pakistan and Tajikistan, Intermediate depth earthquakes were from range 80 – 300 km of 2^{nd} – 8^{th} magnitude. Earth's rotation speed has been acquired from length of day variations of IERS http://hpiers.obspm.fr/eop-pc/ EOP 08 C04 IAU 2000 62-now, html solution. Moon's hour angles and declinations were calculated from Sun and Moon Position Calculator on Internet. Formulas for Schuster's test are given in Heaton (1975) or Tanaka et al. (2002) and many others.

References

Burša, M. (1987a) Secular tidal and non-tidal variations in the Earths rotation. Studia geoph. et geodet., 31, 219–224.

Burša, M. (1987b) Secular deceleration of the Moon and of the Earth's rotation in the zonal geopotential harmonics. Bull. Astron. Inst. Czechosl., 38, no. 5, 309-313.

Cathles, L. M. (1975) The viscosity of the Earth's mantle, Princeton Press, Princeton, NJ.

Heaton, T. H. (1975) Tidal triggering of earthquakes, Geophys. J. R. Astron. Soc., 43, 307-326.

Jeffreys, H. (1975) Tidal friction, Q. J. R. Soc. **16**, 145-151

Kalenda, P., Ostřihanský, L., Rušajová, J. and Holub, K. (2016) The role of tides and LOD in the case of earthquake triggering. Trieste, Conference: G-ET Symposium 06 2016, Affiliation: Trieste University Campus, DOI: **10.13140/RG.2.1.1586.6489**

Lambeck, K. (1977) Tidal dissipation in the oceans: astronomical, geophysical and oceanographic consequences. Philos. Trans. R. Soc. London, 287, pp. 545–594 Ser. A.

Lay, T., Kanamori, H., Ammon, C..J., (2005) The Great Sumatra-Andaman earthquake of 26 December 2004. Science 308(5725) 1127-33.DOI: **10.1126/science/1112250**.

Negredo, A. M., Rephanaz, A. Villasenor, A and Guillot, S. (2006) Evolution of continental subduction in the Pamir-Hindu Kush region: insights from seismic tomography, tectonic reconstructions and numerical modelling, Geophysical Research Abstracts, Vol. 8, 04950, 2006 SRef-ID: 1607-7962/gra/EGU06-A-04950.

Ostřihanský, L. (1991) Forces causing the movement of plates, poster presented at IUGG XX. General Assembly, Vienna, 11–21 August 1991.

Ostřihanský, L. (1997) The causes of lithospheric plates movements, Charles University Prague, Chair of Geography and Geoecology.

Ostřihanský, L., (2010a). Length of a day and the strong Taiwan region earthquake of 26th December 2006. Poster Programme TS10.1/GD3.3, EGU2010-1710, A503..

Ostřihanský, L. (2010b). Length of a day and the L'Aquila earthquake of 6th April 2009, Geophysical Research Abstracts, Vol. 12, EGU2010-1706, 2010, EGU General Assembly 2010

Ostřihanský, L., (2012a). Earth's rotation variations and earthquakes 2010–2011, Solid Earth Discuss., 4, 33–130, https://doi.org/10.5194/sed-4-33-2012,.

Ostřihanský, L., (2012b) Causes of earthquakes and lithospheric plates movement, Solid Earth Discuss., 4, 1411–1483, https://doi.org/10.5194/sed-4-1411-2012,.

Ostřihanský L (2015a) Tides as drivers of plates and criticism of mantle convection, Acta Geod. Geophys., 50, (3), 271-293 doi: **10.1007/s40328-014-0080-6**

Ostřihanský, L., (2015b) Tides as triggers of earthquakes in Hindu Kush. Verification of tidal movement of plates (Available on ResearchGate)

Ostřihanský, L., (2015c) Tides as triggers of earthquakes in Nepal. (Available on ResearchGate) November 2015, DOI: **10.13140/RG.2.1.4340.1681** 2015-11-21 T 13:39:17 UTC

Ostřihanský, L. (2016a) Tides as triggers of earthquakes in Hindu Kush. Verification of tidal movement of plates. (Correction: Moon's azimuths were replaced by Moon's hour angles), Available on ResearchGate,

Ostřihanský, L. (2016b) The correct mechanism of lithospheric plates movement, .Poster at Session Plate motion, Continental Deformation and Intraseismic Strain Accumulation. AGU Fall Meeting 2016 San Francisco 12-16 December 2016.

Ostřihanský, L. (2016c) Verification of tidal earthquake triggering in Central Italy. Poster at Session The 24 August 2016 Earthquake, AGU Fall Meeting 2016 San Francisco 12-19 December 2016.

Ostřihanský, L. (2016d) The next strong earthquake in Central Italy will be in autumn 2034 Poster at Session The 24 August 2016 Earthquake, AGU Fall Meeting 2016 San Francisco 12-19 December 2016.

Ostřihanský, L.. (2017a) The next strong earthquake in South-Central Alaska will be in 2021, Project Earthquake prediction. June 2017, doi**:** **10.13140/RG.2.2.18897.94569.**

Ostřihanský, L. (2017b) Fortnightly dependence of San Andreas tremor and low frequency earthquakes on astronomical parameters, Available on Researchgate..

Ostřihanský, L.. (2018) Verification of tidal earthquake triggering in Taiwan. Doi: **10.13140/RG.2.2.20806.78401**. Available on ResearchGate. .

Ostřihanský, L.. (2019a) Tides as triggers of earthquakes in Sulawesi (Completed). Available on ResearchGate,.

Ostřihanský, L. (2019b). Summary of the most evident tidal actions on solid Earth. Available on Researchgate.

Ostřihanský, L., (2020a). Principles of lithospheric plates movements and earthquakes triggering. Available on ResearchGate.

Ostřihanský, L., (2020b). Collision between India and Asia in light of action of tides., Available on Researchgate, DOI: **10.13140/RG.2.2.36287.12962**

Ostřihanský, L., (2020c). No mantle convection but efficient tidal forces move plates . Available on Researchgate. **doi.org/10.1002/essoar.10505761.1**

Ostřihanský, L., (2021a). Precursors of Haiti earthquakes. Available on Researchgate. DOI: **10.13140/RG.2.2.10757.68327**.

Ostřihanský, L., (2021b). Earthquake prediction for South-Central Alaska has been fulfilled Available on Researchgate DOI: **10.13140/RG.2.2.22659.43041**

Ostřihanský, L., (2022a). No mantle convection and earthquakes 2002 –2021. Available on Researchgate DOI: **10.1002/essoar.10510411.1.**

Ostřihanský, L., (2022b).No mantle convection and enigmatic subduction of oceanic lithosphere. DOI: **T0 1002/essoar.10510998/1** Available on Researchgate.

Ostřihanský, L., (2022c) Phantasmagoria of Earth's mantle convection and correct plates movements. DOI: **10. 1002/essoar/1051.1240.1** Available on Researchgate.

Searle, M., Hacker, B. R. and Bilham, R. (2001) Hindu Kush Seismic Zone as a Paradigm for the Creation of Ultrahigh-Pressure Diamond- and Coesite-Bearing Continental Rocks, Journal of Geology, 109, 143–153.

Searle, M. (2013) Colliding continents, Oxford University press, 433 p.

Stacey, F. D., (2007) Physics of the Earth, John Willey & Sons, 2 Edn.,.

Stein, S. and Okal, A., (2005) Speed and size of the Sumatra earthquake, Nature, 434, 581-582..

Schuster, A. (1897) On lunar and solar periodicities of earthquakes, P. R. Soc. London, 61, 445–465.

Tanaka, S., Ohtake, M., Sato, H., (2002) Evidence for tidal triggering of earthquakes as revealed from statistical analysis of global data, J. Geophys. Res., 107(NO. B10), 2211, doi: **10.1029/2001JB001577**.

Varga, P. and Denis, C. (2010) Geodetic aspects of seismological phenomena, J. Geod., 84, 107–121, doi:10.1007/s00190-009-0350-1,.

Wheeler, R.L., Bufe, C.G., Johnson,M.L.,Dart, R.L., (2005) Seismotectonic Map of Afghanistan with Annotated Bibliography USGSOpen File Repport 2005-1264,31 p.